Gene Therapy (2003) 10, 1067–1078

www.nature.com/gt

RESEARCH ARTICLE

Pancreatic cancer escape variants that evade immunogene therapy through loss of sensitivity to IFNγ-induced apoptosis

G Mazzolini[1], I Narvaiza[1], LA Martinez-Cruz[1,2], A Arina[1], M Barajas[1], JC Galofré[1], C Qian[1], JM Mato[1,2], J Prieto[1] and I Melero[1]

[1]*Gene Therapy Unit, Department of Medicine, School of Medicine, University of Navarra, Pamplona, Spain; and* [2]*Genomic and Proteomic Unit, Department of Medicine, School of Medicine, University of Navarra, Pamplona, Spain*

Combined injections into experimental tumor nodules of adenovirus encoding IL-12 and certain chemokines are capable to induce immune-mediated complete regressions. In this study, we found that the combination of two adenoviruses, one encoding IL-12 and other MIP3α (Ad-CMVIL-12+AdCMVMIP3α) was very successful in treating CT-26-derived colon carcinomas. However, in experimental tumors generated from the pancreatic carcinoma cell line Panc02 such combined treatment induces 50% of macroscopic complete regressions, although local relapses within 1 week are almost constant. We derived cell lines from such relapsing tumors and found that experimental malignancies derived from their inoculum were not amenable to treatment in any case with AdCMVIL-12+AdCMVMIP-3α. Importantly, relapsing cell lines were insensitive to in vitro induction of apoptosis by IFNγ, in clear contrast with the original Panc02 cells. Comparative analyses by cDNA arrays of relapsing cell lines versus wild-type Panc02 were performed revealing an important number of genes (383) whose expression levels were modified more than two-fold. These changes grouped in certain gene ontology categories should harbor the mechanistic explanations of the acquired selective resistance to IFNγ.
Gene Therapy (2003) **10,** 1067–1078. doi:10.1038/sj.gt.3301957

Keywords: *IFNγ; IL-12; MIP3-α; apoptosis; tumor-escape-variants*

Introduction

So far, the most promising gene therapy strategies for cancer are those based upon augmenting the immune response towards tumor antigens.[1,2] Adenovirus-mediated gene transfer of a number of cytokines inside the malignant tissue induces tumor regressions in many models.[1,3] Combinations of more than one of the immunopotentiating genes achieve better results.[1,4–12] Some of such synergistic combinations encompass a chemokine plus a T-cell-activating cytokine to mediate attraction and activation of infiltrating inflammatory cells.[5–7,13] Gene transfer of IL-12 has shown potent antitumor activity by itself[3,14,15] that can be enhanced upon combination with lymphotactin,[16] IP-10[5] or Mig.[5,6] Macrophage inflammatory protein 3α (MIP-3α) is a chemokine mainly secreted by activated macrophages, which interacts with its cognate receptor CCR6 to attract a number of leukocyte types to inflammatory foci with selectivity for tisular dendritic cells (DCs).[17,18] Gene transfer of MIP-3α into experimental tumors has been reported to display antitumor activity and to induce early infiltration by DCs.[19]

Correspondence: Dr G Mazzolini, Gene Therapy Unit, Department of Medicine, School of Medicine, University of Navarra, Avda. Pio XII s/n. 31008 Pamplona, Spain
Received 6 June 2002; accepted 14 November 2002

The most important effector mechanism in these approaches is the generation of cytotoxic T lymphocytes (CTLs) capable of destroying tumor cells. To achieve this goal, CTLs need to recognize specific antigens presented by MHC class-I molecules[20] and to acquire molecular mechanisms capable of destroying tumor cells, such as perforin, Fas-L, as well as secretion of cytokines that induce apoptosis of malignant cells.[21,22] However, the same CTL response can select, among tumor cells, CTL-insensitive variants that have lost antigens,[23,24] antigen-presenting molecules[25] or their susceptibility to the lytic mechanisms.[26,27]

Herein, we describe an experimental pancreatic cancer that relapses because it has lost its susceptibility to IFN-γ-induced apoptosis as a mechanism of escape to gene transfer treatment with IL-12+MIP-3α. This fact underscores the importance of IFN-γ as a major antitumor effector mechanism.[28,29]

Results

Intratumor gene transfer of IL-12+MIP-3α induces intensely immunotherapeutic results

In previous reports by our group and others,[1,3,5–12,34] the activity of intratumoral injections of first-generation recombinant adenovirus encoding IL-12 (AdCMVIL-12) has been extensively described. For our combination studies, a similar adenovirus was constructed encoding

for MIP-3α cDNA under the control of the immediate/early CMV promoter (AdCMVMIP-3α), as schematically represented in Figure 1a. CT26 cells infected with AdCMVMIP-3α at different MOIs released into the tissue culture supernatant a polypeptide recognized by a specific mAb in enzyme immune assays (Figure 1b).

According to the hypothesis of attraction/activation,[7,13] we have combined intratumor IL-12 gene transfer with gene therapy with cDNA encoding for different chemokines. In CT26-derived tumors that had grown for 8 days in syngenic BALB/c mice, intratumor injection of 5×10^8 PFU of AdCMVMIP-3α induced only one out of six complete regressions (Figure 2a). In order to test a possible synergistic effect with IL-12 gene transfer, we used an intratumoral suboptimal dose[5] (7.5×10^7 PFU) of AdCMVIL-12 that induced regression in three out of five tumors. Combined injection of identical doses of both adenoviruses eradicated every tumor (six out of six), indicating the potency of the therapeutic combination, that was confirmed in a repeated experiment shown in Figure 2b in which AdCMVIL-12 (7.5×10^7 PFU)+AdCMVMIP3-α (5×10^8 PFU) caused four out of five tumors to regress, whereas a similar dose of AdCMVIL-12 cured only one out of four. In those two experimental groups receiving

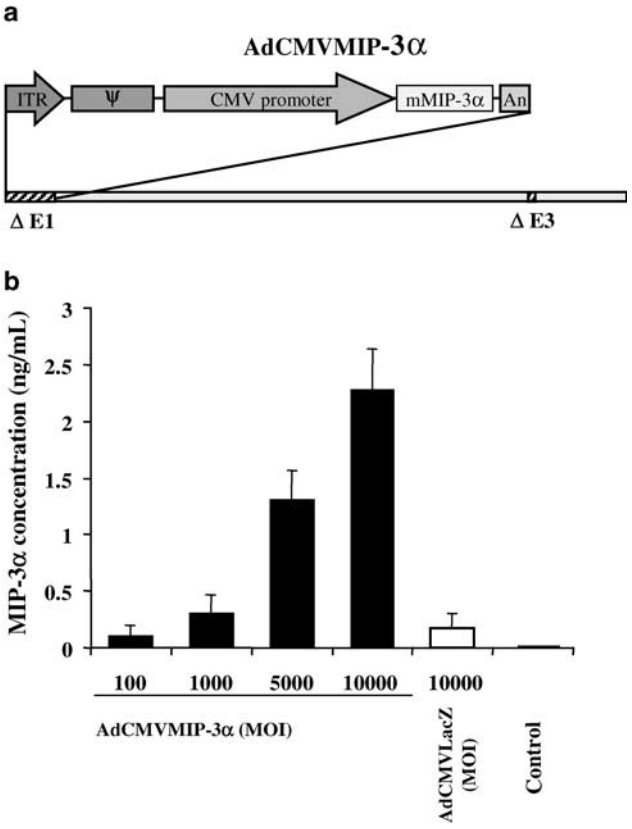

Figure 1 *Construction of AdCMVMIP3-α and in vitro production of the transgene. (a) RT-PCR was used to clone mMIP3-α cDNA from mouse thymus. MIP3-α cDNA was cloned downstream the CMV promoter and upstream polyA signal (An) into adenoviral shuttle vector pSQ1 containing the adenoviral packaging signal (Ψ). pSQ1/MIP-3α and pJM17 were cotransfected into 293 cells by calcium phosphate precipitation generating AdCMVMIP3-α. (b) Direct EIA analysis of MIP3-α production of cell culture supernatants from untransfected CT26 cells (control), infected with AdCMVlacZ (MOI: 10 000) or AdCMVMIP3-α at a MOI of 100, 1000, 5000 and 10 000 as indicated.*

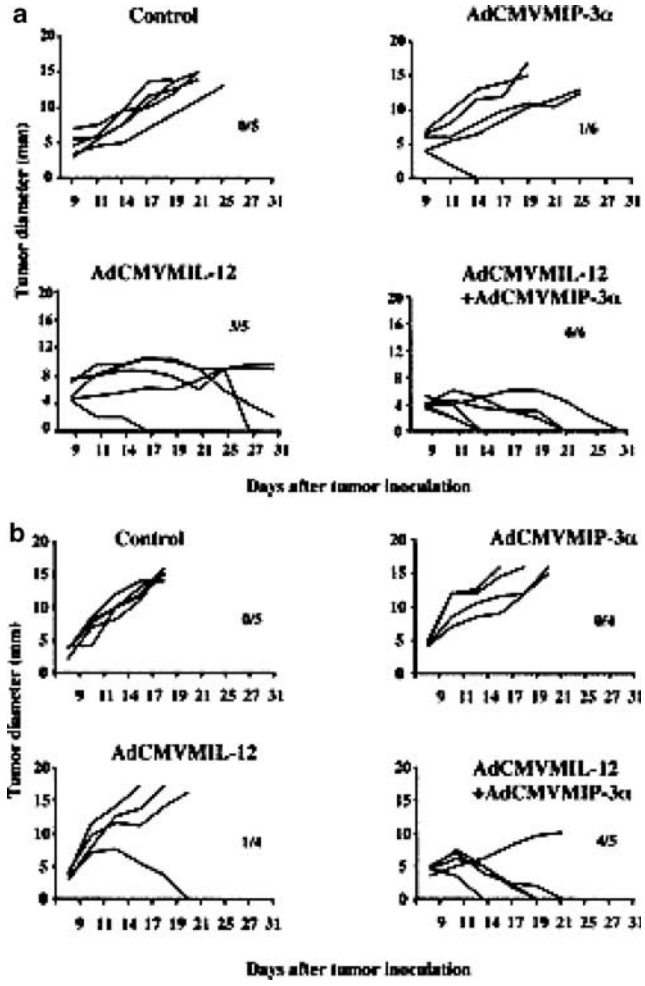

Figure 2 *Intratumor injection of AdCMVIL-12+AdCMVMIP3-α displays a potent and synergistic antitumoral effect on CT26 colorectal carcinomas. BALB/c mice bearing subcutaneous CT26 tumor nodules (4–5 mm in diameter) were injected intratumorally with saline buffer as control, 7.5×10^7 PFU of AdCMVIL-12, 1×10^8 PFU of AdCMVMIP3-α, or a combination of both adenoviruses at identical doses. Data represent follow up of the mean diameter of tumor nodules was assessed every 3 days. The fraction of tumor-free surviving mice 3 months after treatment is given in each panel. Panels a and b represents two different experiments similarly done.*

subtherapeutical i.t. doses of AdCMVIL-12, IL-12 intratumor concentrations were comparable ranging from 2 to 11 pg/mg of tumor tissue at day 4 after treatment. In order to exclude transgene-unrelated antitumoral effects caused by adenovirus combinations, we performed (data not shown) an additional set of experiments combining AdCMVIL-12 (7.5×10^7 PFU)+AdCMVlacZ (5×10^8 PFU) that results in the similarly poor antitumoral effects observed with AdCMVIL-12 alone, thus confirming results that we have published in a previous work performed in the same model.[5]

Intratumor injection of AdCMVIL-12+AdCMVMIP-3α induces transient macroscopic complete regressions of experimental pancreatic carcinomas derived from Panc02 cell line

In our hands, CT26 shows relatively high immunogenicity, since its progression in Rag1$^{-/-}$ BALB/c mice is

much faster than in BALB/c wild-type mice (Tirapu *et al*, manuscript in preparation). Therefore, we moved onto the Panc02 tumor model, which shows lower intrinsic immunogenicity in similar experiments. In Panc02-derived tumors, neither AdCMVIL-12 nor AdCMVMIP-3α displayed any detectable therapeutic activity (Figure 3). By contrast, combination of both adenoviruses induces complete regressions in six out of 12 tumors (three out of six tumors in experiment represented in Figure 3 and three out of six tumors represented in Figure 7). Surprisingly, although tumors remained undetectable by careful palpation and inspection, relapses took place within approximately 1 week after regression in every case. In C57BL/6 Rag1$^{-/-}$ mice, devoid of T and B-cells, this inhibition of growth never did take place (0/6), indicating that the effect was mediated by the adaptative immune system (not shown).

Tumor cell lines derived from relapsing tumors exhibit phenotypic changes including resistance to IFN-γ-induced apoptosis

Tumors experiencing transient regression upon treatment with AdCMVIL-12+AdCMVMIP-3α, that is, those described in Figure 3, were explanted and put into cell culture. Two cell lines derived from Panc02 relapsing tumors were thus generated and named Panc02-A and Panc02-B. It was found that Panc02-WT cells showed different shape and growth pattern *in vitro* compared to Panc02-A and Panc02-B. While Panc02-WT tended to show round aspect and grew in clumped islets, Panc02-A (Figure 4b) and Panc02-B (Figure 4c) grew displaying a fusiform shape and a diffuse pattern of growth over the culture plate (Figure 4). Interestingly, *in vitro* treatment of Panc02-A and Panc02-B with a range of IFN-γ concentrations from 125 to 1000 IU/ml did not cause significant cell death, in marked contrast with Panc02-WT cells, which die within 24–48 h through an apoptotic process (Figure 5a and c).

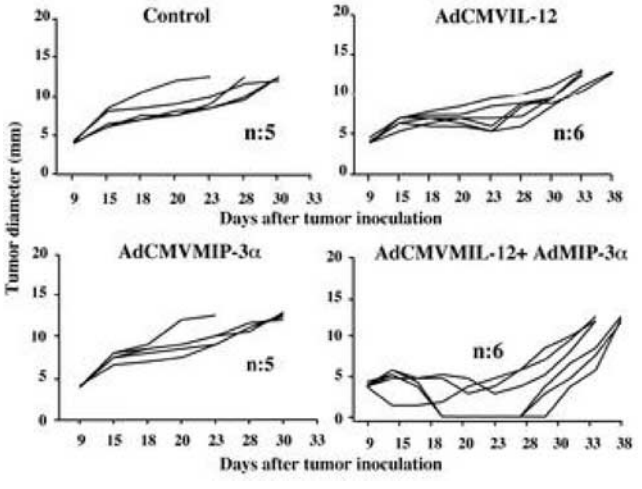

Figure 3 *In vivo gene transfer of IL-12 and MIP-3α induces transient macroscopic complete regressions of subcutaneously implanted pancreatic adenocarcinomas. C57BL/6 mice carrying Panc02 subcutaneous tumor nodules (4–5 mm in diameter) were treated either with saline buffer as control (a), 7.5×10^7 PFU of AdCMVIL-12 (b), 1×10^8 PFU of AdCMVMIP3-α (c), or a combination of both adenoviruses at identical doses (d). Sizes of tumors were measured every 3 days using. Data are representative of two independent experiments.*

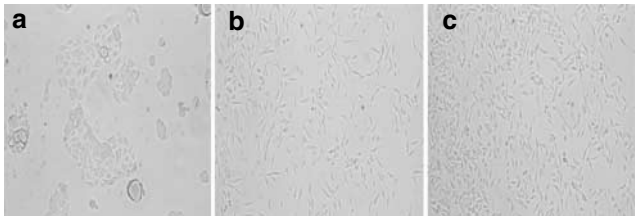

Figure 4 *Tumor cell lines derived from relapsing Panc02 tumors after treatment with AdCMVIL-12+AdCMVMIP3-α exhibit morphological changes. Panc02-WT subcutaneous tumor nodules treated with a combination of AdCMVIL-12+AdMIP3α that had experienced regression were excised aseptically after relapsed and put into cell culture (see Materials and methods). Representative fields of phase-contrast microscopy (×100 magnification) of Panc02-WT (a), and derived cell lines named Panc02-A (b) and Panc02-B (c) are shown. Panc02-WT cells are sphere shaped and grow in clumped islets whereas Panc02-A and B grew displaying a fusiform appearance and displayed a diffuse pattern of growth.*

Under similar conditions, TNF-α failed to induce apoptosis in both Panc02-WT and derived cell lines, suggesting specificity of the differential phenotype (Figure 5b).

Expression of surface IFNγ-receptor was found at similar levels in the three cell lines (Figure 5d). In order to assess whether there were loss of IFN-γ-receptor proximal signal transduction, we measured the ability of IFN-γ to upregulate MHC class-I expression in Panc02-A and Panc02-B. It was found that IFN-γ readily increases H-2K^b levels both in Panc02-A and Panc02-B, as well as in Panc02-WT (not shown and reference 31), indicating the integrity of IFN-γ response at least in this regard (Figure 5e). Cell death induced by IFN-γ in Panc02-WT was not mediated by Fas-FasL interactions since the agonistic anti-Fas mAb Jo-2 failed to induce apoptosis both in Panc02-WT and its derived cell lines, regardless that Fas was detected by FACS analysis on the surface of the three cell lines (not shown). In addition, a neutralizing anti-TRAIL mAb failed to prevent IFNγ-induced death in Panc02-WT (data not shown) that resembles the cytological features of apoptosis (membrane blebbing, cell detachment, presence of apoptotic bodies, etc) absent in similarly treated Panc02-A and B cells (Figure 6a). However Panc02-A and B were as susceptible as Panc02-WT to the induction of apoptosis by UV light irradiation, indicating that the programmed cell death executing machinery was preserved in the tumor escape variants (Figure 6b).

The inevitable occurrence of tumor relapse after treatment with AdCMV-IL12+AdCMVMIP-3α led us to hypothesize that the escaping IFNγ-resistant phenotype could be already present in the polyclonal Panc02-WT cells. Indeed, we found that we could routinely raise IFNγ-resistant cells upon culture of serial dilutions of Panc02-WT in the presence of 1000 IU/ml of the cytokine after 1–2 weeks (not shown).

Panc02-A and Panc02-B variants are resistant to in vivo gene transfer with AdCMVIL-12+AdCMVMIP-3α

The cell lines derived from explanted, relapsing Panc02 tumors were also tumorigenic upon subcutaneous injection in syngenic mice.

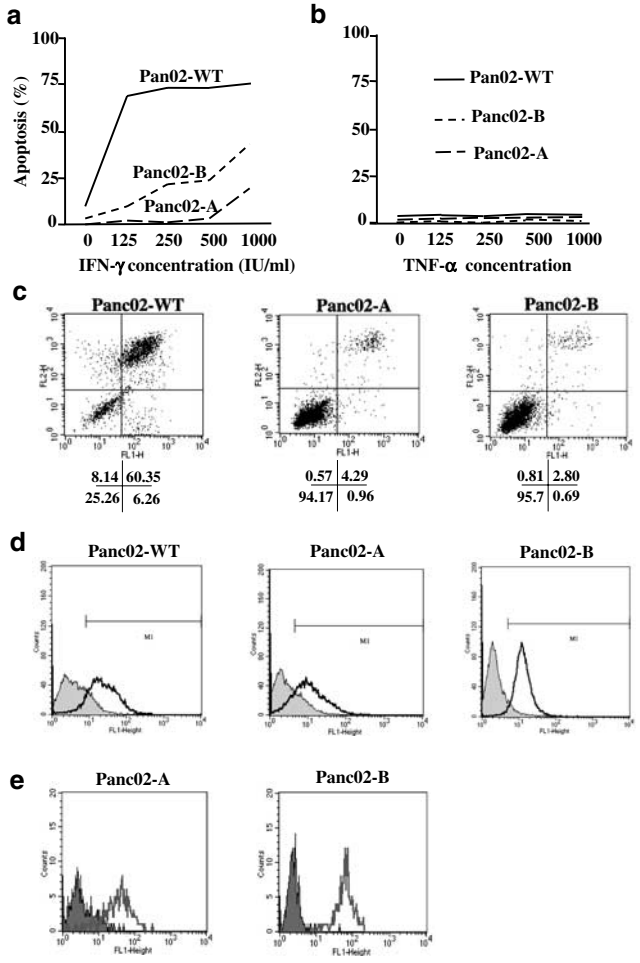

Figure 5 *Panc02-WT-derived cell lines (Panc02-A and Panc02-B) are resistant to IFNγ-induced apoptosis in vitro, but IFNγ increases their level of MHC class-I expression. Panc02-WT and its derived cell lines were plated at 5×10^4 cells/well in 24-well plates. After 24 h, 125, 250, 500 and 1000 IU/ml of IFNγ were added to the cultures. A trypan blue exclusion dye test was performed 2 days later, showing a clear IFNγ dose-dependent apoptosis in Panc02-WT cells, whereas Panc02-A and B appeared to be highly resistant (a). Under similar culture conditions, TNF-α cannot induce apoptosis neither in Panc02-WT nor in derived cell lines (b). (c) FACs analysis of apoptotic dead cells by PI (Fl-2)/annexin V (Fl-1) staining in the indicated cell lines treated with 1000 IU/ml of IFNγ for 24 h. (d) FACS analysis by indirect immunofluorescence of INFγ-receptor expression in Panc02-WT, A and B cultured cell lines. (e) FACs analysis of the specific immunostaining H-2K^b of the indicated cell lines cultured with 1000 IU/ml of IFNγ (solid histograms) or without this cytokine (empty histograms).*

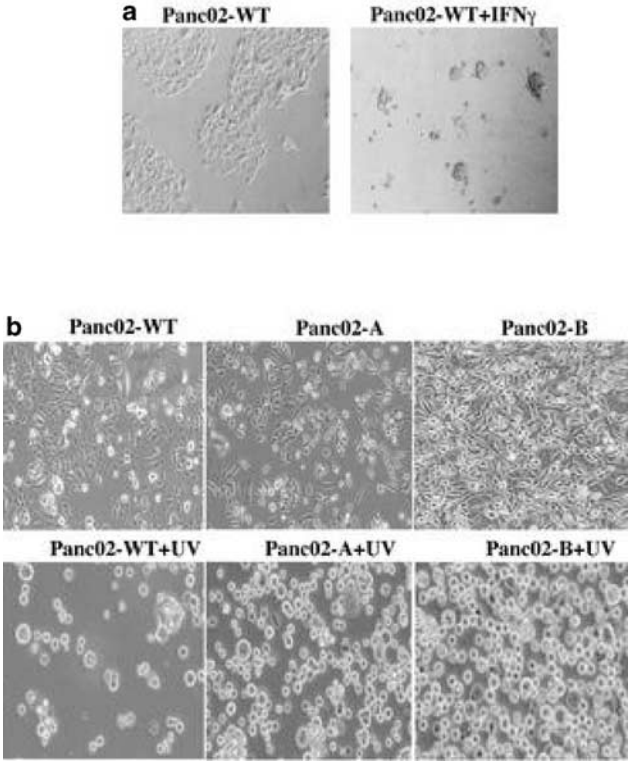

Figure 6 *Panc02-A and B cell lines are resistant to IFNγ-induced apoptosis but susceptible to DNA damage-dependant apoptosis induced by UV light. (a) Phase contrast microscopy pictures (× 100 magnification) of Panc02-WT exposed to 500 IU/ml of rmIFNγ during 48 h (data are representative of 10 experiments similarly performed). (b) Phase-contrast microscopy pictures (× 100 magnification) of Panc02-WT, A and B cells exposed to UV light (0.360 J/cm^2) 12 h prior to the assay.*

However, in contrast to tumors derived from the Panc02-WT cell line (Figure 7a) they were not affected in their growth by intratumoral injection of 7.5×10^7 PFU of AdCMVIL-12+10^8 PFU of AdCMVMIP-3α (Figure 7b and c), although pathological examination of treated tumors disclosed that Panc02-WT showed necrotic areas and leukocyte infiltration, whereas tumors derived from Panc02-A did not show such changes upon the same treatment (not shown).

A potential reason for these differences could be the variable levels of susceptibility to infection by first generation recombinant adenovirus in the different lines. However this reason was ruled out, at least *in vitro*, since comparable levels of *in vitro* gene transduction are achieved when using similar recombinant adenovirus encoding β-galactosidase as a reporter gene (Ad-CMVlacZ) at various MOIs (Figure 7; upper quadrants).

Search for genetic differences in Panc02-WT versus Panc02-A and Panc02-B

In order to explore gene expression changes that could explain the phenotype of resistance to IFNγ-induced apoptosis in the escaping cell lines, we performed cDNA expression arrays (Murine Genome-U74AvZ arrays, Affimetrix), which combined oligonucleotide probes for the whole annotated mouse genome plus 6.000 expression sequence tags (ESTs).

RNA was isolated from cell lines that were 70% confluent during homogeneous, logarithmic, expansion-phase in every cell line. The logics to narrow down the candidate genes to determine the phenotype was to compare gene expression levels in Panc02-WT with Panc02-A and with Panc02-B. The gene or genes responsible for the effect should be up- or down-regulated both in A and B since both cell lines shared the distinct phenotype. Only a limited number of genes was found to be upregulated (91 known genes, and 73 cDNAs or ESTs) or downregulated (137 known genes, and 82 cDNAs or ESTs) more than two times in Panc02-A and Panc02-B in comparison with Panc02-WT, as it can be seen in the dot plot diagram of Figure 8.

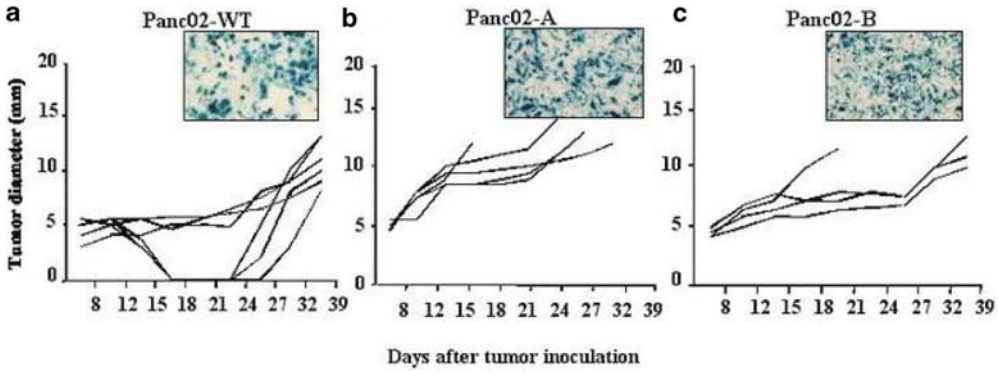

Figure 7 *Panc02-derived cell lines are resistant to gene transfer in vivo with AdCMVIL-12+AdCMVMIP-3α. 2.5×10^5 Panc02-WT (a), Panc02-A (b) and Panc02-B (c) cells were injected subcutaneously in syngenic C57BL/6 mice. When tumors reached a diameter above 4–5 mm, animals were treated intratumorally with 7.5×10^7 PFU of AdCMVIL-12+1 $\times 10^8$ PFU of AdCMVMIP3-α. Data represent follow up of the mean diameter of tumor nodules assessed every 3 days. Data are representative of two independent experiments. Adenoviral transduction efficiency in Panc02-WT, Panc02-A and Panc02-B cells was evaluated in vitro 24 h after infection with a reporter adenovirus (AdCMVlacZ) (MOI: 500) encoding β-galactosidase gene (upper quadrants).*

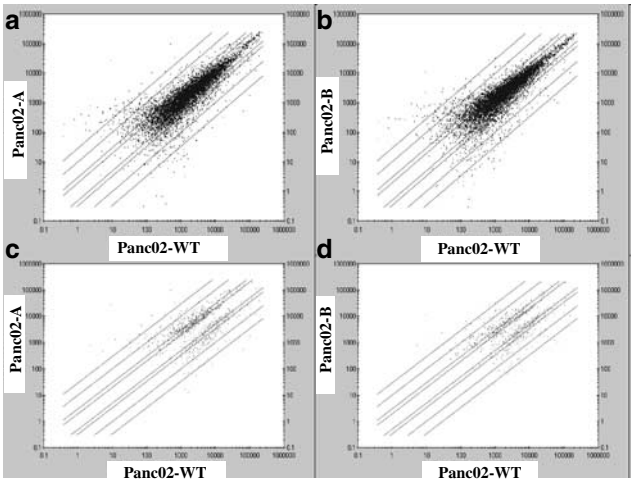

Figure 8 *Genetic differences between Panc02-WT and derived cell lines in cDNA expression arrays. Dot-plot diagram display of the relative intensity of expression of genes analyzed by Affimetrix microarrays in Panc02-A versus Panc02-WT (left) and Panc02-B versus Panc02-WT (right). Lower panels are restricted to genes with two or more fold up- or downregulation.*

From the microarray experiments, one first notices that differential expression profiles are quite similar in both Pan02-A and Pan02-B when compared with Pan02-WT (see Figure 8). However, in Panc02-A *versus* Panc02-WT, the total number of upregulated genes (435) is higher than that of downregulated sequences (382). This tendency is inverted when one compares Pan02-B *versus* Pan02-WT (255 up and 355 down, respectively). Interestingly, the analysis revealed that common up- or downregulated genes cluster mainly in three ontological categories including Cell communication, Cell growth and/or maintenance, and Developmental processes (see Figure 9). Within these groups, genes concentrate in four subcategories, represented by those participating in responses to external stimulus, cell–cell fusion, metabolism and genetic exchange. A complete list of all genes included in each GO category is given as Supplementary Information. Common up- or downregulated genes in Pan02-A and Pan02-B *versus* WT are represented in Figure 9c (left and right, respectively) in which genes were grouped according to the Biological Process in which they are involved[33] (Figure 9). The identity of the genes with the highest changes in the relative levels of expression in Panc02-WT *versus* Panc02-A and B is highlighted in Tables 1 (underexpressed genes) and 2 (overexpressed genes).

The two genes showing the extreme up- and down-fold changes in their levels of expression were analyzed by quantitative PCR to confirm differential expression in Panc02-WT *versus* Panc02-A and Panc02-B. As it can be seen in Figure 10, clusterin RNA was clearly expressed in Panc02-WT whereas it was almost completely lost in Panc02-A and Panc02-B. On the contrary ceruloplasmin RNA levels were much greater in the case of Panc02-A and Panc02-B than in Panc02-WT. However, in this case expression of ceruloplasmin RNA was also detected in Panc02-WT at levels comparable to the housekeeping enzyme GAPDH RNA. In other words, ceruloplasmin seems to have been overexpressed during the transformation of Panc02-WT cells into the escaping variants from basal levels. In the case of clusterin results are compatible with a nearly complete loss of expression. The intensity of the observed changes with clusterin and ceruloplasmin RNA concentrations, that are fully consistent with the cDNA microarray data, suggest a role for these molecules in the apoptotic response to IFNγ.

Discussion

The main findings of this study are: (i) The synergistic antitumoral effect of a combination of recombinant adenovirus, one encoding MIP-3α and the other IL-12 given intratumorally; (ii) that this combination induces macroscopic regression of a number of pancreatic cancers derived from the Panc02 cell line, but relapses take place constantly; (iii) That cell lines derived from such relapsing tumors are insensitive to IFNγ-induced apoptosis *in vitro*, while tumors derived from their inoculation into syngenic mice are completely insensitive to the treatment with AdCMV-IL12+AdCMVMIP-3α. An attempt was also made to identify changes in gene expression responsible for the relapsing phenotype. This

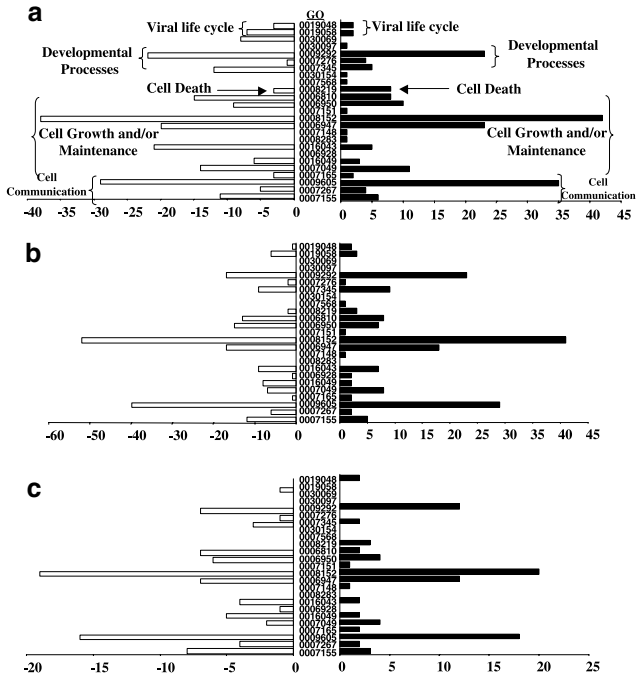

Figure 9 *Database analysis by GO categories of the differential gene expression profile in A and B cell lines versus WT cells: (a) Genes upregulated (black bars) and downregulated (white bars) in A cells versus WT cells; (b) Genes upregulated (black bars) and downregulated (white bars) in B cells versus WT cells; (c) Genes upregulated (black bars) and downregulated (white bars) in A and B cells versus WT cells. GO identification codes for the corresponding Biological Process categories as indicated in the x-axis are: GO: 0008044: adult behavior; GO: 0007626: locomotory behavior; GO: 0007622: rhythmic behavior; GO: 0007155: cell adhesion; GO: 0008037: cell recognition; GO: 0007267: cell–cell signaling; GO: 0009605: response to external stimulus; GO: 0007165: signal transduction; GO: 0007049: cell cycle; GO: 0016049: cell growth; GO: 0006928: cell motility; GO: 0016043: cell organization and biogenesis; GO: 0008283: cell proliferation; GO: 0007148: cell shape and size control; GO: 0006947: cell–cell fusion; GO:0019725: ion homeostasis; GO: 0008152: metabolism; GO: 0007151: sporulation; GO: 0006950: stress response; GO: 0006810: transport; GO: 0008219: cell death; GO: 0007568: aging; GO:0030154: cell differentiation; GO: 0007345: embryogenesis and morphogenesis; GO:0007338: fertilization; GO: 0007276: gametogenesis; GO: 0009292: genetic exchange; GO: 0030097: hemopoiesis; GO: 0007013: actin modification; GO: 0007599: hemostasis; GO: 0019058: viral infectious life; GO: 0019048: virus–host interaction.*

was analyzed by cDNA microarrays disclosing variations in a fairly large number of genes, that interestingly grouped into categories related to cell communication, cell growth and developmental processes when we used an informatic tool that classifies genes according to gene ontology (GO) categories. However, the amount of genes found makes it unfeasible for any approach to single out a phenotype-determining gene (in the eventual case that there existed one).

The idea of combining gene-transfer of a cytokine and a chemokine is not new.[5–7] Several combinations are successful and there exists a rationale behind it, which is described as the 'attraction and activation' theory[7,13]. According to this concept, in our conditions IL-12+MIP3-α probably helps the induction of tumor-reactive T-lymphocytes and their infiltration into malignant tissue.

Gene transfer of both IL-12[3,14,34] and MIP-3α[19] is known to display curative antitumor effects in some murine models. The former cytokine causes T-cell/NK-cell immunity[35] plus antiangiogenesis,[36] while the second is known for its chemoattractive properties for immature DCs that are induced to infiltrate the tumors.[19] Theoretically, those DC take up antigens from malignant cells that are transported to lymphoid tissue in a presentable fashion for responding T-cells. The combination of MIP-3α+IL-12 had the advantage of letting a decrease in the dose of IL-12. This is considered important to avoid the IFNγ-mediated toxicity that is induced by this anticancer agent.[37,38] Efficacy of the MIP-3α+IL-12 combination was comparable to the one displayed by IL-12+IP10 chemokine against the CT-26 colorectal cancer model.[5]

IL-12 key functional feature is its ability to induce IFNγ secretion from T-cells, NK cells as well as DC.[35,39,40] This release of IFNγ is antigen-independent and is related both to its therapeutic effects and to its toxicity.[35] IFNγ is a major factor produced by cytotoxic-T-lymphocytes upon encounter with a target tumor cell presenting cognate antigen.[7,31,41] IFNγ facilitates antigen recognition in surrounding cells by promoting MHC class-I expression[42] and it has been recently described that in several models helps to induce programmed cell death of tumor cell lines.[43–46] Therefore, IFNγ, directly or by indirect mechanisms such as macrophage activation,[41] is a

Table 1 mRNAs underexpressed in Panc02-A and B in comparison to Panc02-WT

	Gene bank accession number	*Fold decrease*	
		Panc02-A	*Panc02-B*
Clusterin	D14077	−55.4	−7.1
CPE-R (*clostridium perfingrens* receptor)	AB000713	−53.9	−17.8
Ly 49D (killer cell lectin-like receptor)	U10090	−32.8	−8.3
Carbonic anhydrase II	M25944	−26.6	−18.7
MAL proteolipid	J07812	−24.7	−20.5
Laminin gamma-2	U43327	−17.2	−12.2
Inhibitor DNA-binding 2 (Id-2)	AF077861	−9.3	−2.2
Leukocyte integrin β (CD18)	M31039	−9	−4.2
Keratin complex-1	M36120	−13.5	−13.9
UcDNA	AA592182	−14.9	−5.1
UcDNA	AW123037	−14.1	−7.3
UcDNA	AW04563	−12.8	−13.9
UcDNA	AW124113	−8.4	−9.8

U: undefined.

Table 2 mRNAs overexpressed in Panc02-A and B in comparison to Panc02-WT

	Gene bank accession number	*Fold increase*	
		Panc02-A	*Panc02-B*
Ceruloplasmin	U49430	73	60
Gas-1 (growth arrest specific 1)	X65128	30	24.9
Leukoprotease inhibitor gene	F002719	17.1	5.5
Xanthine dehydrogenase	X75129	14	13.9
UcDNA	AW208628	11.9	5
Clast-1	AB031386	9.4	5.6
PAF acetylhydrolase	U34277	9	11.3
C/EBP (CCAAT enhancer binding protein)	X61800	8.3	11
Fibulin extracellular matrix glycoprotein	X70853	8.1	11
UcDNA	AW124470	8.1	10.3
Epithelial membrane protein-3	U87948	7.7	10.4

U: undefined.

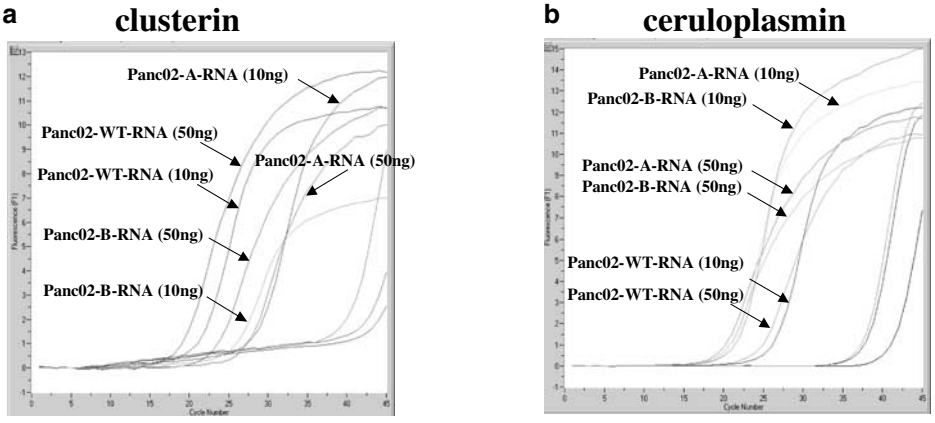

c

		Panc02-WT	Panc02-A	Panc02-B
clusterin	ng specific RNA	1.501±0.05	0.002	0.067±0.020
	ng RNA/ ng RNA GADPH	0.798±0.152	0.001	0.089±0.028
ceruloplasmin	ng specific RNA	2.068±0.208	37.995±3.068	47.039±3.214
	ng RNA/ ng RNA GADPH	1.099±0.110	23.257±1.878	61.978±4.234

Figure 10 *Clusterin and ceruloplasmin RNA levels by real-time RT-PCR (a and b). Real-time RT-PCR curves measuring double-stranded DNA with SYBR Green fluorescence intensity with specific-primers for clusterin (a) and ceruloplasmin (b) plotted with the number of PCR cycles. Curves with each templates are indicated with arrows in the graphs. (c) Table showing RNA-quantitative results that were calculated with standard curves performed as in A and B and referred either as nanograms of specific RNA in 5 μg of total RNA or as a ratio with the quantity of GADPH RNA in each sample. Triplicate samples were analyzed and mean+standard deviation is provided.*

potential effector molecule of the antitumor CTL-response. We found that a pancreatic carcinoma cell line escaped AdCMVIL-12+AdCMVMIP-3α intratumoral therapy precisely because of resistance to IFNγ-induced apoptosis, a prominent feature in the cell line from which they derived (Panc02-WT). The loss of sensitivity to this cytokine appears to be selective, since well-known apoptosis-inducing factors such as TNFα and Fas-L failed to induce apoptosis in both wild-type and derived cell lines. The signal pathway from IFNγ receptor to gene expression control in the nucleus seems preserved, since IFNγ readily upregulated MHC class-I expression in the escaping cell variants as well as in the original cell line. Therefore, a pathway leading to tumor cell death in Panc02-WT is interrupted in Panc02-A and Panc0-B. Moreover, the lost pathway must be independent of the Stat-1, IRS-1 and CIITA-mediated upregulation of MHC class I.[41] In addition, similar levels of mRNA expression for those transcription factors were found in Panc02-WT as well as in A and B variants by microarray analyses (data not shown). Little is known about the signals that promote apoptosis after IFNγ ligation to IFNγR.[47–50] We are currently exploring signal transduction in these particular cells regarding apoptosis induction by IFNγ.

It is possible that the escaping mutant variants were already present in the original Panc02-WT population since *in vitro* culture of these cells in the presence of IFNγ rendered in week-time colonies growing in the presence of 1000 IU/ml of IFNγ. This favors the interpretation that the *in vivo* immunotherapeutic treatment selects out the escaping variants that were already present as a minority among Panc02-WT cells.

To identify candidate changes in genes or in proteins that could explain the resistant phenotype observed in Panc02-derived cell lines, we reasoned that such variations should be overexpressed or underexpressed in both of the escaping cell lines, compared to the wild type. The tools used for this study included analysis of gene-expression from cDNA microarrays encompassing probes for the whole-annotated mouse genome plus a large number of ESTs. This approach narrowed down the number of genes, but still an important number of candidates[51] with significant variation of expression common to both escaping cell lines was substantiated (up=164 and down=219), hence precluding individual study. In a sense the phenotype could be the result of only one of such changes or alternatively the result from the sum of a number of them. We favor the second interpretation and we analyzed the genes by grouping them into ontological categories according to the Biological Process in which they are involved[33] (Martinez-Cruz *et al*, manuscript in preparation that describes the informatics of algorithms functioning on the databases). Similar classification criteria have been used to analyze complete genomes[52] and changes of gene expression profiles in transgenic mice.[53]

From the list of genes with up- or downregulation in Panc02-A and Panc02-B *versus* Panc02-WT some of them had striking fold changes and are the subject of our current and future research. For instance, among underexpressed genes we find clusterin (fold changes A *versus* WT: −55.4; B *versus* WT: −7.1). This gene has been involved both in promotion and protection from apoptosis with a still elusive molecular mechanism.[54,55] Curiously the receptor for *Clostridium perfringens enterotoxin* (CPE-R) is decreased in its expression (−53.9-fold in A and −17.8-fold in B). This gene is a target for pancreatic cancer therapy and its function as a putative transmembrane channel makes it very interesting since its physiological role is still unknown.[56] Carbonic anhydrase II, MAL protelipid, laminin γ2 were also genes with more than 10-fold downregulation in both escaping cell lines and deserve future study for their potential role at changing IFNγ susceptibility and/or cell shape of the tumor cells.

On the contrary, other genes were drastically upregulated among them: ceruloplasmin (73-fold and 60-fold in A and B, respectively), Gas 1 (growth arrest specific 1) (fold 30/24.9), xanthine deshydrogenase (14/13.9). These genes have not obvious involvement in the observed phenotype, but novel functions could be discovered for them. Furthermore, ceruloplasmin and xanthine dehydrogenase have a role in the defense against oxidative stress[57] that may be involved in the observed resistance to apoptosis. Besides, platelet activatory factor (PAF) acetylhydrolase is also upregulated (nine times in A/11.3 times in B); this is also an interesting finding since it has been recently proposed that this molecule might have implications in tumor biology.[58]

It has been recently shown that small changes in expression results in severe disease.[59] Therefore, excessive focusing in the highlighted changes could be misleading since it cannot be excluded that genes with small changes may play key roles in promotion and/or protection from apoptosis. Nonetheless the role played by those extreme fold changes in the levels of RNA encoding for clusterin and ceruloplasmin, that have been confirmed by quantitative PCR, is the matter of our current research efforts.

We think that other alterations not involving changes in mRNA expression, such as point mutations that might alter the function due to production of nonfunctional proteins, should not be overlooked. These changes are not addressed by the analysis of cDNA arrays. In addition, an important number of sequences corresponding to ESTs and cDNAs without assigned function were differentially expressed in Panc02-WT and escaping malignant cells. It is possible that a key piece of information is still missing due to insufficient gene function knowledge.

In conclusion, beyond describing a successful immunotherapeutic gene combination, this study raises a new concern for immunity-based gene therapy, since it adds a novel mechanism of tumor escape through the acquisition of resistance to IFNγ-induced apoptosis. Our attempt to study the gene expression profile of escape variants showed variation in multiple genes that tend to group in certain functional categories. Our ongoing and future research tries to identify the master switch changes in gene expression that would hierarchically explain the phenotype of the escaping-malignant cells.

Material and methods

Mice and cell lines

At 5- to 8-week-old C57BL/6 ($H2^b$) and BALB/c ($H2^d$) female mice were purchased from Harlan (Barcelona, Spain) and were housed according to institutional guidelines. The 293 cell line was obtained through American Type Culture Collection (ATCC) (Manassas, VA, USA). CT26 tumor cell line is an undifferentiated murine colorectal adenocarcinoma.[14] The mouse pancreatic cancer Panc02 was established in C57BL/6 mice induced by 3-methylcholantrene and presented as a ductal pancreatic adenocarcinoma.[30,31] The subcutaneous Panc02 tumor tissue was obtained from the National Cancer Institute, DCTDC Tumor Repository (Frederick, MD, USA). A cell line was isolated from trypsination of Panc02 tumor tissue. Panc02 and CT26 cells were maintained in RPMI 1640 medium containing 10% FCS, 2 mM L-glutamine, 100 U/ml streptomycin, 10 μg/ml ciprofloxacin and 100 μg/ml penicillin. Cell culture reagents were from Life Technologies (Basel, Switzerland).

Adenovirus construction

The mouse MIP-3α cDNA was generated by an RT-PCR technique using total RNA extracted from mouse thymus as template with primers (sense: 5′-ACCATGGCCTGCGGTGGCAAGCGT-3′ and antisense: 5′-GATATCTTACATCTTCTTGACTCTTAG-3′) and directly cloned into pCR2.1-TOPO (Invitrogen, Carlsbad, CA, USA). The sequence was confirmed by DNA sequencing.

The MIP-3α sequence was cloned into adenoviral shuttle vector pSQ1 with CMV immediate/early promoter upstream and polyA sequence downstream of the insertion site to form pSQ1/MIP-3α. pSQ1/MIP-3α and pJM17 were cotransfected into 293 cells by calcium phosphate precipitation to obtain AdCMVMIP-3α according to standard procedures.[14] Recombinant adenoviruses carrying the p40 and p35 genes of IL-12 (AdCMVIL-12) or β-galactosidase (AdCMVlacZ) under the control of CMV promoter have been previously described.[32] Adenoviruses were purified by double cesium chloride ultracentrifugation and extensively dialyzed against 10 mM Tris/1 mM $MgCl_2$ prior to be stored at $-80^{\circ}C$ in the presence of 10% (v/v) glycerol. Titration was made by plaque assay.[32]

In vitro MIP-3α production

Supernatants from AdCMVMIP-3α-infected CT26 cells (3×10^5 cell/well in 12-well plates) at MOIs 100 and 10 000, as well as noninfected CT26 cells, were collected 48 h after infection. MIP-3α levels were measured by direct enzyme immunoabsorbent assay (EIA). A 96-well flat-bottomed microtitration plate (Titertek, ICN Biochemicals INC. Aurora, OH, USA) were coated with 100 μl of different supernatants and standards in identical medium (recombinant murine MIP-3α, R&D Systems, Minneapolis, MN, USA) and maintained at 4°C overnight. The plates were washed five times with 100 μl phosphate-buffered saline (PBS)-Tween (0.05%) and blocked with 100 μl of PBS containing 10% fetal bovine serum (FBS) for 2 h at room temperature. After blocking, the plates were washed in PBS-Tween and incubated for 2 h at room temperature with 100 μl of anti-mouse MIP-3α (R&D Systems) at final concentration of 2 μg/ml. The plates were washed five times and further incubated in PBS-Tween with 10% FBS containing 100 μl of 1:2000 diluted peroxidase-conjugated anti-goat IgG (SIGMA, Madrid, Spain). After 2 h of incubation at room temperature, the plates were washed 10 times with 100 μl of PBS-Tween. Color was developed with 100 μl of tetramethylbenzidine substrate (BD Biosciences Pharmingen, San Diego CA) followed by 50 μl of stop solution (2 N H_2SO_4). Absorbance (OD) of samples was read by a Titertek Multiscan II (Flow Laboratories) microplate reader at 450 nm. Results were determined in duplicate and expressed as the mean ± s.d.

Establishment of subcutaneous model in vivo

Prior to administration of treatment, BALB/c and C57BL/6 mice were inoculated s.c. in the right hind flank with 5×10^5 CT26 or 2.5×10^5 Panc02-WT tumor cells in 50 μl of PBS. For treatment, when tumors reach a diameter above 4–5 mm, subcutaneous tumors were injected with 50 μl of PBS containing 7.5×10^7 PFU of AdCMVIL-12, 5×10^8 PFU of AdCMVMIP-3α or both. Similarly, tumors derived from Panc02-A and Panc02-B cell lines were treated with 7.5×10^7 PFU of AdCMVIL-12+5×10^8 PFU of AdMIP3α or saline. Tumor size (mean diameter) was assessed using a precision caliper.

Tumor cell lines derived from relapsing tumors

Panc02-WT tumors treated with 7.5×10^7 PFU of AdCMVIL-12+5×10^8 PFU of AdMIP3α that experienced regression and subsequent relapse were excised aseptically and single-cell suspensions were obtained passing the cells through a mesh and then put into cell culture. Culture medium was RPMI 1640 supplemented with 10% FCS, 2 mM L-glutamine, 100 U/ml streptomycin, 10 μg/ml ciprofloxacin and 100 μg/ml penicillin. The two cell lines derived were named Panc02-A and Panc02-B. Cell culture reagents were from Life Technologies (Basel, Switzerland).

In vitro IFN-γ-induced apoptosis

Panc02-WT, Panc02-A and Panc02-B cells were plated at 5×10^4 cells/well onto 24-well plates (Greiner Labortechnik) and cultured in RPMI 1640 medium to subconfluence. After 24 h, cells were incubated at different concentrations (100–1000 IU/ml) of mrIFN-γ (Peprotech. UK). 36 hs after exposure to IFNγ, Tripan blue dye exclusion test was carried out. UV light induction of apoptosis was performed by exposure at 0.360 J/cm^2 during 60 s in a DNA cross linker device (UVItec CL508G).

Detection of major histocompatibility complex (MHC) class-I expression

Suspensions of Panc02-WT, Panc02-A and Panc02-B were tested for H-2K^b expression by flow cytometry analysis. Cells were washed with PBS and stained with FITC-tagged mAb anti-H-2K^b (Pharmingen, San Diego, CA, USA). Indirect immunofluorescence staining with anti-IFNγ-receptor mAb (Pharmingen) was developed with FITC-tagged polyclonal anti-rat IgG (Sigma, Barcelona, Spain). Control staining with irrelevant FITC-tagged rat mAb was also used. After washing, cells were analyzed using flow cytometer (Facscallibur, Becton-Dickinson).

FACS analysis of apoptotic cells by annexin-V staining

To detect and quantify apoptosis of both Panc02-WT and derived cell lines (Panc02-A and Panc02-B) after exposure to rmIFNγ at the indicated concentrations cells were stained with Anexin-V-FLUOS Staining kit (Boheringer Mannheim, Germany) according to the manufacturer instructions.

In vitro transduction of Panc02-WT, Panc02-A and Panc02-B cell lines. X-gal staining

We evaluated the *in vitro* transduction efficiency of the recombinant adenovirus in Panc02-WT, Panc02-A and Panc02-B cells using AdCMVlacZ vector. 10^5 cells in 1 ml of complete RPMI 1640 medium were seeded in 24-well plates. After 24 h, cells were infected at different multiplicities of infection (100, 500 and 1000) with AdCMVlacZ and incubated at 37°C and 5% CO_2 for 48 h. For X-gal staining, cells were fixed in 24-well plates with glutaraldehyde (0.5%) and stained with 5-bromo-4-chloro-3-indoyl-beta-galactosidase (X-Gal) as previously described.[32] The experiment was done twice and triplicates were included.

Gene expression analysis by microarrays

Murine pancreatic cancer Panc02-WT and its derived Panc02-A and Panco2-B cell lines were grown as monolayer in RPMI 1640 supplemented with 10% FCS, 2 mM L-glutamine, 100 U/ml streptomycin, 10 μg/ml ciprofloxacin and 100 μg/ml penicillin. Cells were grown at 37°C in humidified 5% CO_2 atmosphere, placed in 15-cm plates and harvested when at 70–80% confluence.

Total RNA was isolated using the Trizol RNA isolation method (Gibco/BRL) and purified with the Qiagen RNeasy Mini Kit spin columns (Qiagen). RNA concentration was determined using a spectrophotometer. RNA integrity was confirmed on a 1% agarose gel electrophoresis.

Target preparation

Double-strand DNA was synthesized using the Superscript Choice System (Gibco/BRL). In all, 10 μg of total RNA was used in a reverse transcription reaction to synthesize negative strand cDNA with a primer containing poly-T and T7 RNA polymerase promoter sequences. Double-stranded cDNA was phenol–chloroform extracted and ethanol precipitated. The cDNA was resuspended in 12 μl of RNase-free water and 5 μl of the double-stranded cDNA was used as a template for *in vitro* transcription, in the presence of biotinylated UTP and CTP, to generate labeled antisense RNA. The *in vitro* transcription reaction was performed using the Enzo BioArray High Yield RNA Transcript Labeling Kit (Enzo Diagnostics). Labeled RNA was purified with the Qiagen RNeasy Mini Kit spin columns (Qiagen) and quantified spectrophotometrically.

Array hybridization and scanning

Labeled cRNA was fragmented in fragmentation buffer (5× buffer: 200 mM Tris-acetate (pH 8.1)/500 mM KOAc/150 mM MgOAc) and hybridized to the microarrays in 200 μl of hybridization solution containing 15 μg of labeled target in 1× Mes buffer (0.1 M Mes/1.0 M NaCl/0.01% Tween20/20 mM EDTA) and 0.1 mg/ml herring sperm DNA. Test2 arrays (Affymetrix) were hybridized to check the cRNA integrity before the expression arrays and in all cases the GADPH 3′/5′ ratio was below 1.1. Samples were then hybridized on Murine Genome-U74Av2 Arrays (Affymetrix, USA). This array represents all sequences (~6000) in the Mouse UniGene database (Build 74) that have been functionally characterized and ~6000 EST clusters. Arrays were rotated at 60 rpm for 16 h at 45°C. Following hybridization, the arrays were washed with 6× SSPE-T (0.9 M NaCl/60 mM NaH_2PO_4/6 mM EDTA/0.01% Tween20) at 25°C on a fluidics station (Affymetrix) for 10×2 cycles, and subsequently with 0.1 M Mes/0.1 M NaCl/0.01% Tween20 at 50°C for 4×15 cycles. The arrays were then stained with a streptavidin–phycoerythrin conjugate (Molecular Probes), followed by 10×4 wash cycles. To enhance the signals, the arrays were further stained with Anti-streptavidin antibody for 10 min, followed by a 10-min staining with a streptavidin–phycoerythrin conjugate. After 15×4 additional wash cycles, the arrays were scanned using a confocal scanner (Affymetrix). The image data were analyzed by Microarray Suite 4.0 (Affymetrix).

Genechip analysis

Using oligonucleotide microarrays, we studied gene expression profiles of Panc02-A and Panc02-B cell lines *versus* Panc02-WT cells, and analyzed those genes sharing a common up- or downregulation behavior in the microarray experiments. Those differentially expressed genes for which a GO code[33] is assigned in the Unigene database (http://www.ncbi.nlm.nih.gov/Locuslink), were classified according to the Biological Process in which they participate (Martinez-Cruz *et al*, a manuscript in preparation that describes the informatics of algorithms functioning on the databases). Only entries showing an expression fold change equal or bigger than 2.0 were considered.

A complete list of all genes included in each GO category is given as Supplementary Information.

Real-time quantitative RT-PCR

5 μg of total RNA from Panc02-Wt, Panc02-A and Panc02-B cell lines were DNase I treated (1.2 U/μg RNA) before cDNA synthesis. One μg of DNase I treated RNA was used for cDNA synthesis (20 μl) with SuperScript™ Rnase H-Reverse Transcriptase (Invitrogen) (400 U/μg RNA) and 100 pmol oligodT.

Sequences for forward and reverse primers for each gene are the following: 5′CGACTCGCTCCAGGTGGC CGAGAGGC3′ and 5′CCACCTCAGTGACACGGGAGG GGACCTCTGAGT3′ for clusterin; 5′CCTGGTAATCC TACAGATGGACAGAGCAAC3′ and 5′TGGTTTTAGAG CTTTATTGTAGGAAGGCAG3′ for ceruloplasmin; 5′AA GGCTGGGGCTCACCTGAA3′ and 5′GGCATGGACTG TGGTCATGAG 3′ for GAPDH.

A standard curve, with serial dilutions of cDNA, was constructed for each sequence. Template concentrations for reactions in the relative standard were given arbitrary values of 10, 5, 2.5, 1.25, 0.625, 0.3125 and 0.15625.

Real time PCR reactions were prepared using LightCycler-FastStart DNA master SYBR Green I kit (Roche) according to the manufacturer instructions. The amplification program consisted of 1 cycle of 95°C with 1 min hold ('hot start') followed by 45 cycles of 95°C (denaturation) with 10-s hold, 60°C (annealing) with 5-s hold, 72°C (amplification and acquisition) with 10-s hold. Melting curve analysis using the program run for one cycle at 95°C with 0-s hold, 65°C with 15-s hold, and 95°C with 0-s hold at the step acquisition mode followed amplification.

The average of triplicate data of each sample was used to calculate the relative change in gene expression after normalization target concentration to GAPDH.

Acknowledgements

We thank Dr Bendandi and Tirapu for critical reading and helpful discussion. Juan Percaz, Javier Guillen, Izaskun Gabari and Celia Gomar are acknowledged for their technical assistance. The team at Medplant Genetics is acknowledged for assistance with the microarray technology. Financial support was from CICYT (SAF 99/0039), Gobierno de Navarra and grants from Fundación Ramón Areces and Inés Bemberg.

References

1 Melero I *et al*. IL-12 gene therapy for cancer: in synergy with other immunotherapies. *Trends Immunol* 2001; **22**: 113–115.
2 Dranoff GM, Mulligan RC. Gene transfer as cancer therapy. *Adv Immunol* 1995; **58**: 417–454.
3 Bramson JL *et al*. Direct intratumoral injection of an adenovirus expressing interleukin-12 induces regression and long-lasting immunity that is associated with highly localized expression of interleukin-12. *Hum Gene Ther* 1995; **7**: 1995–2002.

4 Emtage PC *et al*. A double recombinant adenovirus expressing the costimulatory molecule B7-1 (murine) and human IL-2 induces complete tumor regression in a murine breast adenocarcinoma model. *J Immunol* 1998; **160**: 2531–2538.
5 Narvaiza I *et al*. Intratumoral coinjection of two adenoviruses, one encoding the chemokine IFN-gamma-inducible protein-10 and another encoding IL-12, results in marked antitumoral synergy. *J Immunol* 2000; **164**: 3112–3122.
6 Palmer K *et al*. Combined CXC chemokine and interleukin-12 gene transfer enhances antitumor immunity. *Gene Ther* 2001; **8**: 282–290.
7 Dilloo D *et al*. Combined chemokine and cytokine gene transfer enhances antitumor immunity. *Nat Med* 1996; **2**: 1090–1095.
8 Putzer B *et al*. Interleukin 12 and B7-1 costimulatory molecule expressed by an adenovirus vector act synergistically to facilitate tumor regression. *Proc Natl Acad Sci USA* 1997; **94**: 10889–10894.
9 Putzer BM *et al*. Large nontransplanted hepatocellular carcinoma in woodchucks: treatment with adenovirus-mediated delivery of interleukin 12/B7.1 genes. *J Natl Cancer Inst* 2001; **93**: 472–479.
10 Martinet O *et al*. Immunomodulatory gene therapy with interleukin 12 and 4-1BB ligand: long-term remission of liver metastases in a mouse model. *J Natl Cancer Inst* 2000; **92**: 931–936.
11 Zitvogel L *et al*. Interleukin-12 and B7.1 co-stimulation cooperate in the induction of effective antitumor immunity and therapy of established tumors. *Eur J Immunol* 1996; **26**: 1335–1341.
12 Addison CL *et al*. Intratumoral coinjection of adenoviral vectors expressing IL-2 and IL-12 results in enhanced frequency of regression of injected and untreated distal tumors. *Gene Ther* 1998; **5**: 1400–1409.
13 Levitsky HI. The best cytokine for the job. *Nat Med* 1997; **3**: 126.
14 Mazzolini G *et al*. Regression of colon cancer and induction of antitumor immunity by intratumoral injection of adenovirus expressing interleukin-12. *Cancer Gene Ther* 1999; **6**: 514–522.
15 Barajas M *et al*. Gene therapy of orthotopic hepatocellular carcinoma in rats using adenovirus coding for interleukin 12. *Hepatology* 2001; **33**: 52–61.
16 Emtage PC *et al*. Adenoviral vectors expressing lymphotactin and interleukin 2 or lymphotactin and interleukin 12 synergize to facilitate tumor regression in murine breast cancer models. *Hum Gene Ther* 1999; **10**: 697–709.
17 Luster AD. Chemokines – chemotactic cytokines that mediate inflammation. *N Engl J Med* 1998; **338**: 436–445.
18 Greaves DR *et al*. CCR6, a CC chemokine receptor that interacts with macrophage inflammatory protein 3alpha and is highly expressed in human dendritic cells. *J Exp Med* 1997; **186**: 837–844.
19 Fushimi T, Kojima A, Moore MA, Crystal RG. Macrophage inflammatory protein 3alpha transgene attracts dendritic cells to established murine tumors and suppresses tumor growth. *J Clin Invest* 2000; **105**: 1383–1393.
20 Hellstrom I, Hellstrom KE. T cell immunity to tumor antigens. *Crit Rev Immunol* 1998; **18**: 1–6.
21 Berke G. Unlocking the secrets of CTL and NK cells. *Immunol Today* 1995; **16**: 343–346.
22 Yagita H *et al*. Role of perforin in lymphocyte-mediated cytolysis. *Adv Immunol* 1992; **51**: 215–242.
23 Seliger B, Maeurer MJ, Ferrone S. Antigen-processing machinery breakdown and tumor growth. *Immunol Today* 2000; **21**: 455–464.
24 Marincola FM, Jaffee EM, Hicklin DJ, Ferrone S. Escape of human solid tumors from T-cell recognition: molecular mechanisms and functional significance. *Adv Immunol* 2000; **74**: 181–273.
25 Garrido F *et al*. Implications for immunosurveillance of altered HLA class I phenotypes in human tumours. *Immunol Today* 1997; **18**: 89–95.
26 Bergmann-Leitner ES, Abrams SI. Influence of interferon gamma on modulation of Fas expression by human colon carcinoma cells and their subsequent sensitivity to antigen-specific CD8+ cytotoxic T lymphocyte attack. *Cancer Immunol Immunother* 2000; **49**: 193–207.
27 Bergmann-Leitner ES, Abrams SI. Positive and negative consequences of soluble Fas ligand produced by an antigen-specific CD4(+) T cell response in human carcinoma immune interactions. *Cell Immunol* 2001; **209**: 49–62.
28 Kaplan DH *et al*. Demonstration of an interferon gamma-dependent tumor surveillance system in immunocompetent mice. *Proc Natl Acad Sci USA* 1998; **95**: 7556–7561.
29 Shankaran V *et al*. IFNgamma and lymphocytes prevent primary tumour development and shape tumour immunogenicity. *Nature* 2001; **410**: 1107–1111.
30 Corbett TH *et al*. Induction and chemotherapeutic response of two transplantable ductal adenocarcinomas of the pancreas in C57BL/6 mice. *Cancer Res* 1984; **44**: 717–726.
31 Clary BM *et al*. Inhibition of established pancreatic cancers following specific active immunotherapy with interleukin-2 gene-transduced tumor cells. *Cancer Gene Ther* 1997; **4**: 97–104.
32 Qian C, Bilbao R, Bruna O, Prieto J. Induction of sensitivity to ganciclovir in human hepatocellular carcinoma cells by adenovirus-mediated gene transfer of herpes simplex virus thymidine kinase. *Hepatology* 1995; **22**: 118–123.
33 Ashburner M *et al*. Gene ontology: tool for the unification of biology. The Gene Ontology Consortium. *Nat Genet* 2000; **25**: 25–9.
34 Caruso M *et al*. Adenovirus-mediated interleukin-12 gene therapy for metastatic colon carcinoma. *Proc Natl Acad Sci USA* 1996; **93**: 11302–11306.
35 Trinchieri G. Interleukin-12: a cytokine at the interface of inflammation and immunity. *Adv Immunol* 1998; **70**: 83–243.
36 Sgadari C, Angiolillo AL, Tosato G. Inhibition of angiogenesis by interleukin-12 is mediated by the interferon-inducible protein 10. *Blood* 1996; **87**: 3877–3882.
37 Robertson MJ *et al*. Immunological effects of interleukin 12 administered by bolus intravenous injection to patients with cancer. *Clin Cancer Res* 1999; **5**: 9–16.
38 Leonard JP *et al*. Effects of single-dose interleukin-12 exposure on interleukin-12-associated toxicity and interferon-gamma production. *Blood* 1997; **90**: 2541–8.
39 Grohmann U *et al*. Positive regulatory role of IL-12 in macrophages and modulation by IFN-gamma. *J Immunol* 2001; **167**: 221–227.
40 Munder M, Mallo M, Eichmann K, Modolell M. Murine macrophages secrete interferon gamma upon combined stimulation with interleukin (IL)-12 and IL-18: a novel pathway of autocrine macrophage activation. *J Exp Med* 1998; **187**: 2103–2108.
41 Sad S, Marcotte R, Mosmann TR. Cytokine-induced differentiation of precursor mouse CD8+ T cells into cytotoxic CD8+ T cells secreting Th1 or Th2 cytokines. *Immunity* 1995; **2**: 271–279.
42 Boehm U, Klamp T, Groot M, Howard JC. Cellular responses to interferon-gamma. *Annu Rev Immunol* 1997; **15**: 749–795.
43 Shyu RY, Su HL, Yu JC, Jiang SY. Direct growth suppressive activity of interferon-alpha and -gamma on human gastric cancer cells. *J Surg Oncol* 2000; **75**: 122–130.
44 Ruiz-Ruiz C, Munoz-Pinedo C, Lopez-Rivas A. Interferon-gamma treatment elevates caspase-8 expression and sensitizes human breast tumor cells to a death receptor-induced mitochondria-operated apoptotic program. *Cancer Res* 2000; **60**: 5673–5680.
45 Wu AJ *et al*. Interferon-gamma induced cell death in a cultured human salivary gland cell line. *J Cell Physiol* 1996; **167**: 297–304.
46 Suk K *et al*. Interferon gamma (IFNgamma) and tumor necrosis factor alpha synergism in ME-180 cervical cancer cell apoptosis and necrosis. IFNgamma inhibits cytoprotective NF-kappa B through STAT1/IRF-1 pathways. *J Biol Chem* 2001; **276**: 13153–13159.
47 Veldman RJ, Klappe K, Hoekstra D, Kok JW. Interferon-gamma-induced differentiation and apoptosis of HT29 cells: dissociation of (glucosyl)ceramide signaling. *Biochem Biophys Res Commun* 1998; **247**: 802–808.

48 Lee KY, Anderson E, Madani K, Rosen GD. Loss of STAT1 expression confers resistance to IFN-gamma-induced apoptosis in ME180 cells. *FEBS Lett* 1999; **459**: 323–326.
49 Jiang MC *et al*. IRF-1-mediated CAS expression enhances interferon-gamma-induced apoptosis of HT-29 colon adenocarcinoma cells. *Mol Cell Biol Res Commun* 2001; **4**: 353–358.
50 Naujokat C, Sezer O, Possinger K. Tumor necrosis factor-alpha and interferon-gamma induce expression of functional Fas ligand on HT29 and MCF7 adenocarcinoma cells. *Biochem Biophys Res Commun* 1999; **264**: 813–819.
51 Wu TD. Analysing gene expression data from DNA microarrays to identify candidate genes. *J Pathol* 2001; **195**: 53–65.
52 Dwight SS *et al*. Saccharomyces Genome Database (SGD) provides secondary gene annotation using the Gene Ontology (GO). *Nucleic Acids Res* 2001; **30**: 69–72.
53 Martínez-Chantar ML *et al*. Spontaneous oxidative stress and liver tumors in mice lacking methionine adenosyltransferase 1A. *FASEB J* 2002; **16**: 1292–2004.
54 Han BH *et al*. Clusterin contributes to caspase-3-independent brain injury following neonatal hypoxia-ischemia. *Nat Med* 2001; **7**: 338–343.
55 McLaughlin L *et al*. Apolipoprotein J/clusterin limits the severity of murine autoimmune myocarditis. *J Clin Invest* 2000; **106**: 1105–1113.
56 Michl P *et al*. Claudin-4: a new target for pancreatic cancer treatment using Clostridium perfringens enterotoxin. *Gastroenterology* 2001; **121**: 678–684.
57 de Silva DM, Aust SD. Ferritin and ceruloplasmin in oxidative damage: review and recent findings. *Can J Physiol Pharmacol* 1993; **71**: 715–720.
58 Bussolati B *et al*. PAF produced by human breast cancer cells promotes migration and proliferation of tumor cells and neoangiogenesis. *Am J Pathol* 2000; **157**: 1713–1725.
59 Yan H *et al*. Small changes in expression affect predisposition to tumorigenesis. *Nat Genet* 2002; **30**: 25–6.